

## Detection of Modulated Wave Transmission Failure in Aviation Communication Using IoT-Based RTL-SDR

Indra Fadillah Mukti, M. Arif Sulaiman\*, M. Faisal Yoga Dewantara

Politeknik Penerbangan Indonesia Curug  
Tangerang-Banten, Indonesia

\*arif.sulaiman@ppcurug.ac.id

**Abstract** – Communication is a crucial component in aviation telecommunications services, where failures can lead to fatal incidents that may result in loss of life. According to Regulation No. 48 of 2017, aviation telecommunication service providers must be able to provide VHF A/G services with an availability value of 0.99999 and detect failures within two seconds. At Perum LPPNPI Yogyakarta, the VHF A/G equipment is located in a transmitter building 760 meters away from the Technician Standby Building. This distance makes it difficult for technicians to directly monitor the equipment's condition, leading to failures being identified based on reports from air traffic controllers. Therefore, the author designed an IoT-based RTL-SDR system to directly monitor equipment conditions based on the modulated waves transmitted. This design employs the ADDIE method in its development. The system operates by measuring the transmission power and audio level of the modulated waves. Based on research conducted at frequencies 120.2 MHz, 125 MHz, 126.7 MHz, 127 MHz, 129.5 MHz, 130 MHz, 132.5 MHz, 133.2 MHz, 134 MHz, and 135 MHz, this design can detect equipment failures based on the received modulated waves with highest and lowest deviation while measuring transmission power are 2.24 dB and 0.4 dB.

**Keywords** – Aviation Communication; IoT-Based Monitoring; RTL-SDR; Modulated Wave Detection; Transmission Power Analysis.

### I. INTRODUCTION

COMMUNICATION is a crucial component in aviation telecommunication services. Failures in aviation telecommunication services can lead to fatal incidents and are one of the major contributors to casualties in aviation accidents [1]. Perum LPPNPI, as the provider of aviation telecommunication services in Indonesia, holds the responsibility for conducting aviation communication services [2]. One of the communication services provided by Perum LPPNPI is air-to-ground communication using Very High Frequency Air to Ground (VHF A/G) equipment. VHF A/G is an aviation communication equipment that transmits radio waves at frequencies of 118 – 137 MHz with Line of Sight (LOS) propagation characteristics [3,4]. According to the Indonesian Ministry of Transportation Regulation No. 48 of 2017 on Civil Aviation Safety Regulation Part 171 concerning the Provision of Aviation Telecommunication Services, aviation telecom-

munication service providers must be able to provide air-to-ground communication services with an availability value of 0.99999 and must detect failures in air-to-ground communication within less than two seconds [5].

At Perum LPPNPI Yogyakarta Branch, the transmitter used by the Approach Control (APP) unit has a transmission power of less than or equal to 50 watts in an omnidirectional pattern and has a channel spacing of 25 kHz or 8.33 kHz [4]. It is located in the Transmitter Building, which is 760 meters from the Technician Standby Building. This distance poses a challenge for technicians to monitor the equipment condition directly, as the equipment status can only be identified through the LED indicator on the front panel of the VHF A/G equipment. Thus, technicians need time to identify failures in the equipment. Currently, technicians receive information from air traffic controllers if there is a failure in the VHF A/G equipment. In response, the researcher proposed designing a failure detection system capable of detecting failures in air-to-ground communication equipment and providing real-time failure information to technicians.

Similar research has been conducted by Cahyani

The manuscript was received on August 3, 2024, revised on November 1, 2024, and published online on November 29, 2024. Emitor is a Journal of Electrical Engineering at Universitas Muhammadiyah Surakarta with ISSN (Print) 1411 – 8890 and ISSN (Online) 2541 – 4518, holding Sinta 3 accreditation. It is accessible at <https://journals2.ums.ac.id/index.php/emitor/index>.

et al. in their study titled “Design of Transmitter Equipment Monitoring for Very High Frequency PAE T6T Based on Web Server” [6]. In that study, the equipment condition was determined by sampling the voltage from the LED indicator on the front panel of the VHF A/G equipment. However, this design could only monitor the equipment condition through the LED indicator on the VHF A/G equipment. Therefore, the researcher is interested in creating a failure detection system with a different approach, using Software Defined Radio (SDR).

SDR is a technology that utilizes software to process information within radio waves [7]. With SDR, users can flexibly modify and extract information from radio waves, such as frequency, signal level, Signal to Noise Ratio (SNR), and more [8]. This flexibility is advantageous as users can easily reconfigure the program to meet desired goals, making SDR usage very versatile [9]. One of the SDR devices is RTL-SDR, which is widely used in applications such as FM radio reception (87.5 MHz – 108 MHz), aeronautical (108 MHz – 117 MHz), meteorological (117 MHz), and more [10, 11].

Research conducted by Molina-Tenorio et al. titled “Real-Time Implementation of Multiband Spectrum Sensing Using SDR Technology” found that RTL-SDR has high accuracy in reading radio signal parameters. Their research involved reading power and SNR at frequencies of 90.6 MHz - 92.8 MHz and 826 MHz – 850 MHz. The measurements showed a deviation (error) of 2% with a data processing speed of 100 ms [12].

In research by Harianto et al. titled “Low Cost Prototype Simulation of Spectrum Analyzer Base on GNU Radio and RTL-SDR,” they compared power and SNR measurements at frequencies of 60 MHz – 80 MHz using RTL-SDR and a Spectrum Analyzer. The results showed that RTL-SDR has very high accuracy, with power measurement accuracy of 99.47% and SNR measurement accuracy of 99.78% [13].

Other studies by Majumder [14] titled “Energy Detection Spectrum Sensing on RTL-SDR Based IoT Platform” and Mohamed et al. [15] titled “Partial Discharge Detection Using Low Cost RTL-SDR Model for Wideband Spectrum Sensing” also aimed to measure the sensitivity and precision of RTL-SDR in reading signal level differences at various frequencies. These studies yielded similar results, showing that RTL-SDR has high sensitivity in signal detection, allowing it to read signal parameter values accurately.

In this study, the author designed a real-time failure detection system for VHF A/G equipment using IoT-based RTL-SDR 2832U. This design works by receiving modulated waves transmitted by the VHF A/G

equipment. The modulated waves received by the RTL-SDR are then processed to produce the transmission power and the audio level values carried by the wave. However, these waves are only processed when the VHF A/G is in transmit mode, which is detected when the user presses the PTT button, sampled using an INA 226 sensor.

The program on the Raspberry Pi determines the transmission status based on these two pieces of information according to the specified parameters. According to the Standard Operating Procedures (SOP) for Aviation Telecommunication Services at Perum LPP-NPI Yogyakarta Branch, modulated waves transmitted by the VHF A/G equipment are considered to trigger an alarm if the signal attenuation exceeds 3 dB from the commissioning value or if they do not carry voice information [16]. The information about transmission power, transmission status, and alarm status is then forwarded to the cloud server via the Raspberry Pi. This system provides real-time alerts to technicians if the received transmission power falls below the tolerance value or if the transmitted modulated wave does not carry voice information.

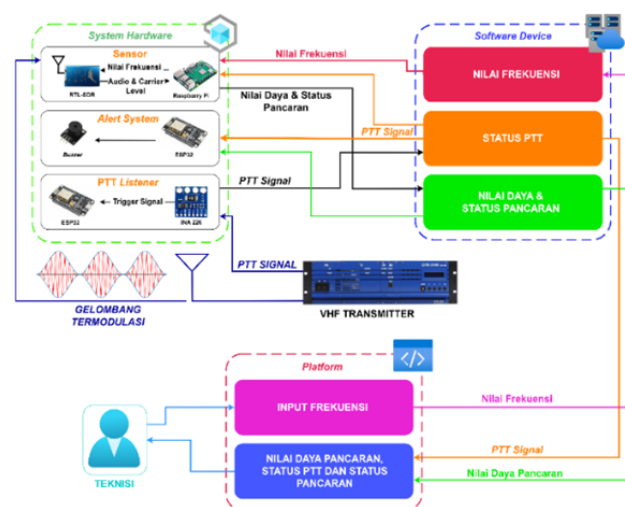


Figure 1: Workflow of the proposed design

## II. RESEARCH METHODS

The ADDIE method is a series of systematic research steps. The process in the ADDIE method consists of Analyze, Design, Development, and Evaluation [17].

### i. Analyze

The first stage in the ADDIE method is analyze. At this stage, a literature review related to the research to be conducted is performed. This research refers to the IoT architecture consisting of system hardware, software device, communication route, and platform [18].

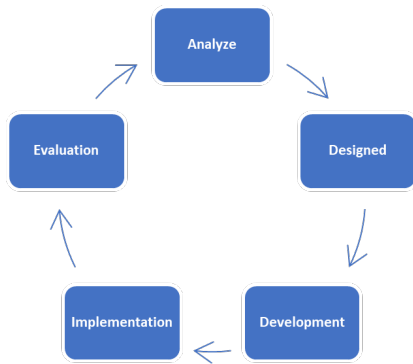


Figure 2: ADDIE Method Workflow

In the system hardware section, a literature review is conducted on SDR devices capable of processing modulated waves transmitted by VHF A/G equipment. Based on KP 103 of 2015, the following are the characteristics of VHF A/G transmissions:

Table 1: Characteristics of VHF A/G Transmissions

Parameter	Value
Operating Frequency	118-137 MHz
Type of Modulation	Amplitude Modulation
Modulation Input	300 – 2500 Hz

ii. Design

After analyzing the needs for hardware and software, the next step is the design phase, which includes components such as the communication route, cloud service, SDR, alert system, PTT listener, and platform. The communication route defines the form of communication between the devices within the system. This system consists of three hardware components: the alert system, which functions as an alarm system; the SDR, which acts as a radio wave detector; the PTT listener, which detects the transmit position of the VHF A/G equipment; and one software component, the platform, which serves as the user interface to the system.

The type of communication used in this system is Wi-Fi, so each hardware device needs to be connected to an access point to access the internet. All communication within the system is centralized in the Firebase Realtime Database, so communication between devices must go through Firebase. The communication between devices and Firebase is two-way in the form of respond and request. The format and type of data sent from the devices to Firebase and vice versa will be discussed in the cloud service section.

The cloud service used in this study is Firebase, which uses a routing system for data storage [19, 20]. In this study, the researcher defined seven routes. The

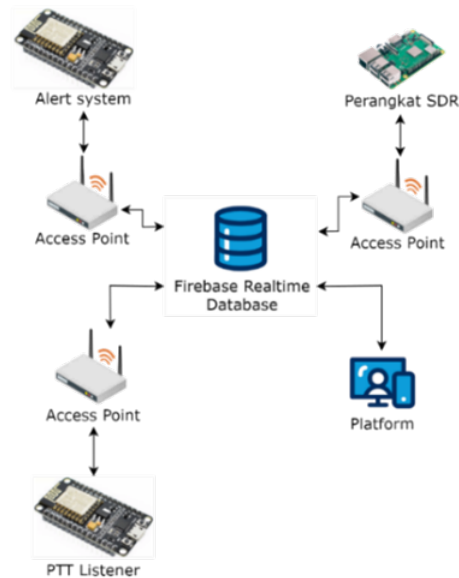


Figure 3: Communication Route

first is “/frekuensi” with a float data type, which stores the operating frequency value of the equipment; “/kalibrasi/n\_val” with a float data type, which stores the transmission power calibration value; “/kalibrasi/status” with an integer data type, which stores the calibration status; “/vhf/ptt” with an integer data type, which stores the transmit position value read by the PTT listener; “/vhf/sdr” with a float data type, which stores the attenuation value detected by the SDR; “/vhf/status” with an integer data type, which stores the transmission status value sent by the alert system; and “/vhf/alarm” with an integer data type, which stores the alarm status value sent by the SDR program.

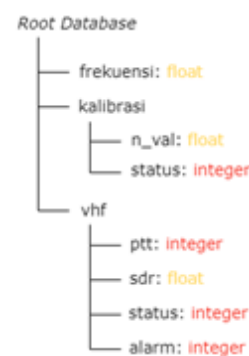


Figure 4: Database Structure

SDR acts as a radio wave detector. This device consists of RTL-SDR and a Raspberry Pi. The developed algorithm is written in Python and created using GNU Radio and Visual Studio Code. GNU Radio is an open-source software capable of building algorithms that can process electromagnetic wave data directly [21]. This algorithm has five input variables: “c\_freq” as the operating frequency, “cal” as the calibra-

tion status, “c\_val” as the normal transmission power value from calibration, and “samp\_rate” as the sample rate value of RTL-SDR.

The algorithm operates by retrieving information at the “c\_freq” frequency. This information is passed through the Complex to Mag2 block to obtain the transmission power value. Additionally, it is passed through the Low Pass Filter and Complex to Mag blocks to obtain the audio signal carried by the carrier wave. Using the Multiply block, the audio signal level is calculated. Based on the information on transmission power and audio signal level, the algorithm determines the transmission status and alarm status, then sends them to the cloud service along with the transmission power value.

**Table 2:** Pseudocode for RF Wave Detector

Pseudocode 1: RF Wave Detector
Input: c_freq, operating frequency cal, calibration status c_val, normal transmission power samp_rate, sample rate Output: rf_power, transmission power value status_p, transmission status status_a, alarm status
<pre> 1. if cal is True, then: 2.   Start listening to c_freq at samp_rate. 3.   Use Complex to Mag2 block to get transmission power. Store in receive_level. 4.   if receive_level &gt; -3dB, then: 5.     Use Low Pass Filter and Complex to Mag blocks to get voice info. 6.     Use Multiply block to get audio level. Store in audio.level. 7.     if audio.level &gt; 0, then: 8.       status_p: normal 9.       status_a: 0 10.      send status_p and status_a to the database 11.     else: 12.       status_p: no information 13.       status_a: 1 14.      send status_p and status_a to the database 15.   else: 16.     status_p: transmission power below tolerance 17.     status_a: 1 18.     send status_p and status_a to the database 19.   else: 20.     start calibration process.           </pre>

The alert system is a device that warns the user when an alarm occurs. This device works by receiving the transmission status information from the cloud service via an ESP32 microcontroller and sounding a buzzer if an alarm status is detected. Additionally, this device has LED indicators and an OLED display to provide information to the user. The algorithm for the alert system is developed using the C++ programming language.

PTT Listener is a device used to sample PTT voltage. This is aimed at determining the transmit position of the VHF A/G equipment. This device utilizes an INA226 voltage sensor to read the voltage value on the PTT. Through this reading, the transmit position of the VHF A/G equipment can be determined. This reading result is then sent to the cloud service.

In this study, the researcher used NextJS as a framework and JavaScript programming language to build the platform. This platform serves as the user interface between the system and the user. The platform consists of four pages: sign-in page, home page,

**Table 3:** Pseudocode for Alert System

Pseudocode 2: Alert System
Input: pttState, PTT status r_stat, transmission status a_stat, alarm status power, transmission power value freq, operating frequency Output: n_led, normal status LED indicator ae_led, no voice status LED indicator rfe_led, RF Power < -3 dB status LED indicator nn_led, normal connection LED indicator ne_led, connection error LED indicator bz, buzzer pin
<pre> 1. if connection is normal, then: 2.   set \HIGH" on nn_led. 3.   Retrieve freq from the database and store in variable freq. 4.   if pttState is True, then: 5.     Retrieve power from the database and store in variable power. 6.     Retrieve r_stat from the database and store in variable r_stat. 7.     Display freq, pttState, power, and r_stat on the OLED. 8.     if a_stat is 0, then: 9.       set \HIGH" on n_led. 10.      set \LOW" on bz. 11.      display \normal" on OLED 12.     else: 13.       set \HIGH" on bz. 14.     if r_stat indicates no information, then: 15.       set \HIGH" on ae_led. 16.       set \LOW" on bz. 17.       display \no audio" on OLED 18.     else if r_stat: RF Power &lt; -3 dB, then: 19.       set \HIGH" on rfe_led. 20.       set \LOW" on bz. 21.       display \RF power drop" on OLED 22.   else: 23.     Display freq and pttState on OLED. 24.   else: 25.     while count &lt;= 10, then: 26.       wifi.reconnect(). 27.       count += 1 28.     ESP.restart().           </pre>

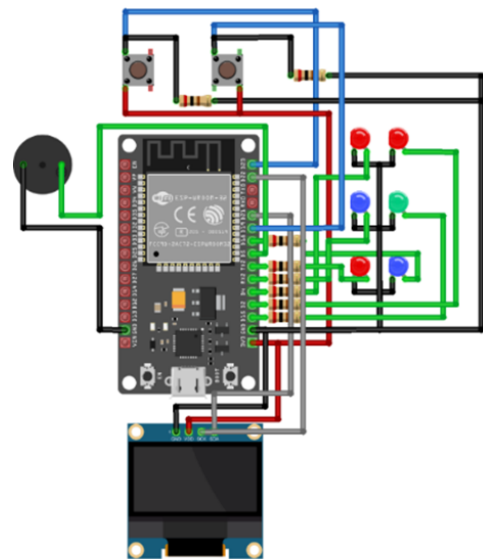


**Figure 5:** Wiring of the alert system

monitor page, and history page.

The home page is the first page displayed when the user accesses the application. This page can be accessed by both authenticated and unauthenticated users. It only displays general information such as the application name and version. This page includes a sign-in button that redirects the user to the sign-in page for authentication.

**Table 4:** Pseudocode for PTT Listener

**Pseudocode 3: PTT Listener**

```

Input: pttVolt, PTT voltage value
state, PTT status (pressed/released)
prev_state, last PTT status
Output: nn_led, normal connection LED indicator
ne_led, connection error LED indicator

1. if connection is normal, then:
2.   Read PTT voltage and store in pttVolt.
3.   if pttVolt is greater than or equal to 12, then:
4.     Set state to 0.
5.   else:
6.     Set state to 1.
7.   while state == prev_state:
8.     Read PTT voltage and store in pttVolt.
9.     if pttVolt is 0, then:
10.      Set state to 1.
11.     else:
12.      Set state to 0.
13.     Send state to the database.
14.   else:
15.     while count <= 10, then:
16.       wifi.reconnect().
17.       count += 1
18.     ESP.restart().
    
```

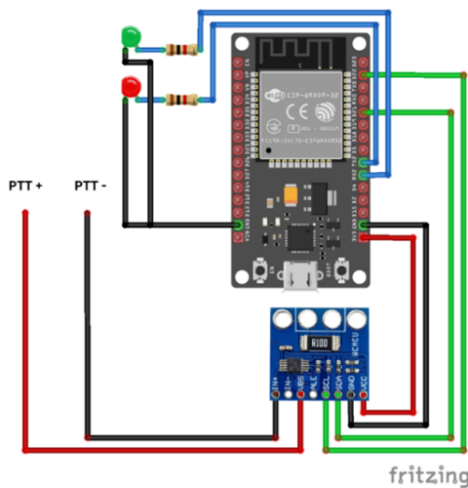


**Figure 6:** Wiring of the PTT listener



**Figure 7:** Layout of the home page

The sign-in page has two input fields: e-mail and password. These inputs are used for user authentication to access the application. The e-mail and password entered by the user are sent to Firebase Authentica-

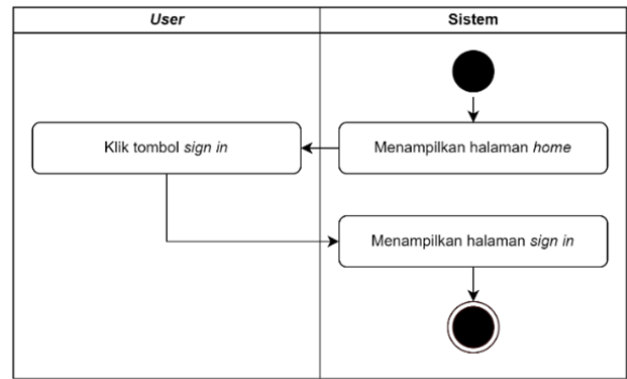


**Figure 8:** Activity diagram of the home page

tion for the authentication process. If authentication is successful, the user is redirected to the monitor page.

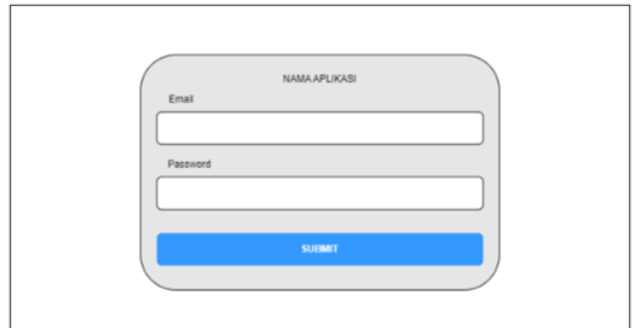


**Figure 9:** Layout of the sign-in page

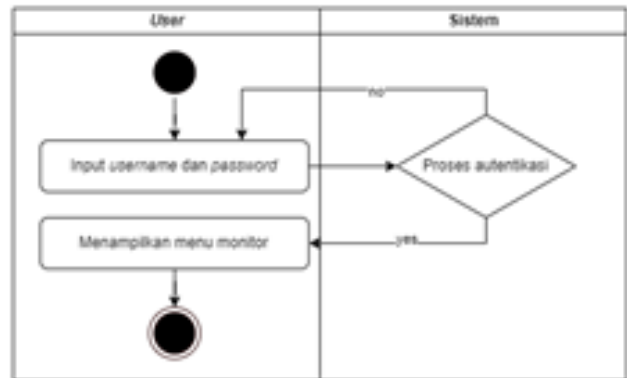


**Figure 10:** Activity diagram of the sign-in page

The monitor page displays the results of SDR readings. Through this page, users can view transmission status, the attenuation value of the transmission, the number of alarms that occurred each month over the past year, and the history of failures. Additionally, users can change the operating frequency on this page.

The history page displays the history of equipment failures. Through this page, users can view failures that occurred in a specific month and print the failure list as a PDF file.

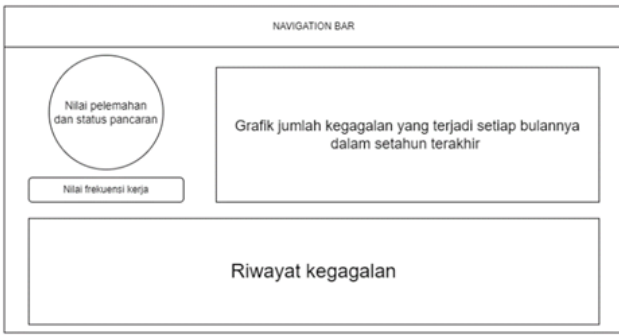


Figure 11: Layout of the monitor page

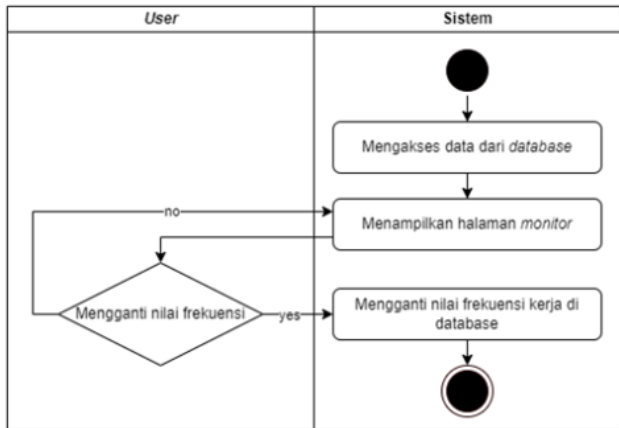


Figure 12: Activity diagram of the monitor page

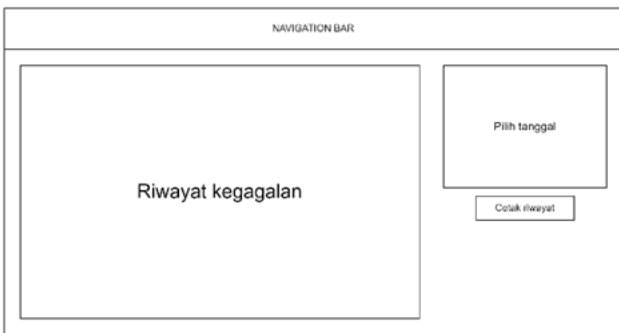


Figure 13: Layout of the history page

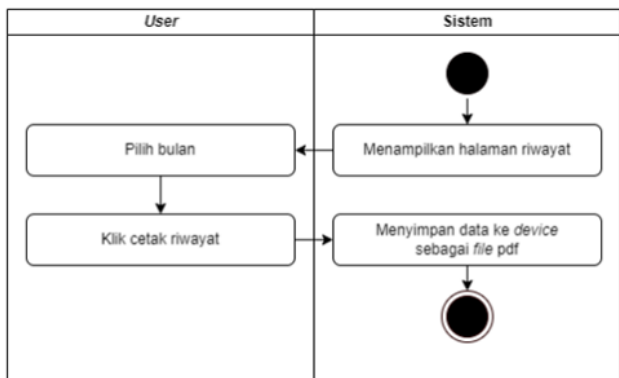


Figure 14: Activity diagram of the history page

iii. Development

In this phase, the author developed the cloud service, SDR, alert system, and PTT listener, which had

been designed in the previous phase. In this study, the researcher used three Firebase features: Real-time Database, Firestore, and Authentication. The researcher created seven database routings to store sensor data: “/frequency,” “/kalibrasi/n\_val,” “/kalibrasi/status,” “/vhf/alarm,” “/vhf/ptt,” “/vhf/sdr,” and “/vhf/status.”

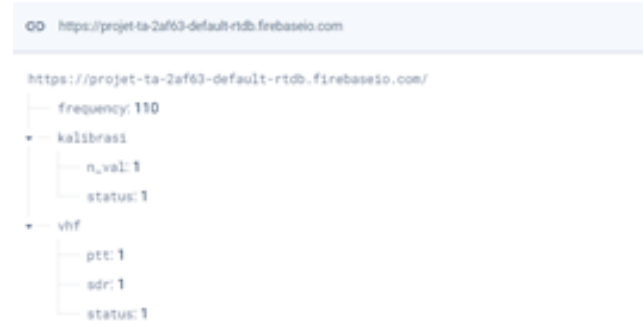


Figure 15: Database routing display

For the SDR section, the author developed the algorithm using GNU Radio and Visual Studio Code. The software development employed a modular programming system, dividing the program into several parts. In this design, the main program was divided into three parts: main.py, firebase\_function.py, and am\_receiver.py.

The am\_receiver.py program was created using GNU Radio. The input for this program is the VHF A/G transmission wave received by the antenna, and the output is the audio level and transmission power value. Once the program is assembled, click run in GNU Radio, then click generate to create a .py file.



Figure 16: Block code in GNU Radio

The firebase\_function.py program includes an algorithm for connecting to Firebase and functions needed to read and write data in Firebase. This program has 11 different functions. The function “getFreq()” reads the operating frequency stored in the “/frequency” routing. The function “changeFreq()” updates the operating frequency stored in the “/frequency” routing. The function “getStatusCal()” reads the calibration status in the “/kalibrasi/status” routing. The function “getCalVal()” reads the normal transmission power calibration value stored in “/kalibrasi/n\_val.” The function “setCalVal()” updates the normal transmis-

sion power calibration value in “/kalibrasi/n\_val.” The function “setStatVal()” updates the calibration status in “/kalibrasi/status.”

The main.py program is the main program that runs the entire SDR function. It integrates fire-base\_function.py and am\_receiver.py. This program retrieves the audio level and transmission power from am\_receiver.py. The received transmission power is then compared logarithmically to the normal transmission power calibration value to obtain the attenuation value. Based on the attenuation and audio level, main.py determines the transmission status and alarm status of the VHF A/G equipment and sends them to Firebase using the “setError()” function.

For the alert system, the hardware was developed using a double-sided PCB measuring 5 x 7 cm. The ESP32 microcontroller used in this design was programmed using Arduino IDE. The developed algorithm required two additional libraries: “U8g2lib” for the display and “Firebase\_ESP\_Client” for ESP32 and Firebase communication.



**Figure 17:** Alert system hardware

For the PTT listener, the hardware was also developed using a double-sided PCB measuring 5 x 7 cm. The ESP32 microcontroller in this design was programmed using Arduino IDE. The developed algorithm required two additional libraries: “INA226\_WE” for reading voltage from the INA226 sensor and “Firebase\_ESP\_Client” for ESP32 and Firebase communication.

The platform used in this project is a web-based application built using the NextJS framework and JavaScript programming language. The application has four pages: home page, sign-in page, monitor page, and history page.

The home page is the first page accessed by the user, as it is located in the root directory. This page displays general information about the application and has three navigation buttons that direct the user to the home, monitor, and history pages, as well as a sign-in

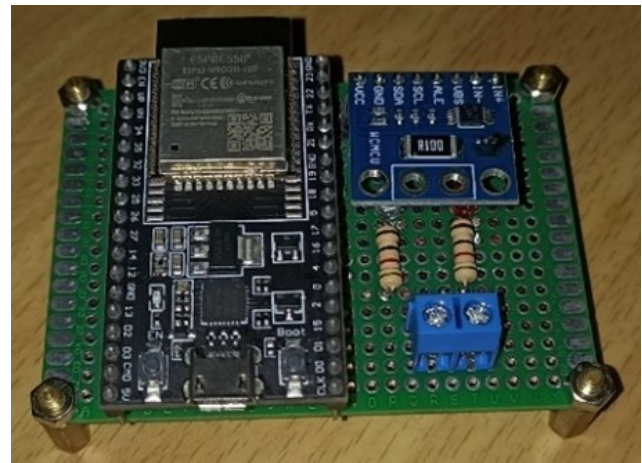


**Figure 18:** PTT listener hardware

button.

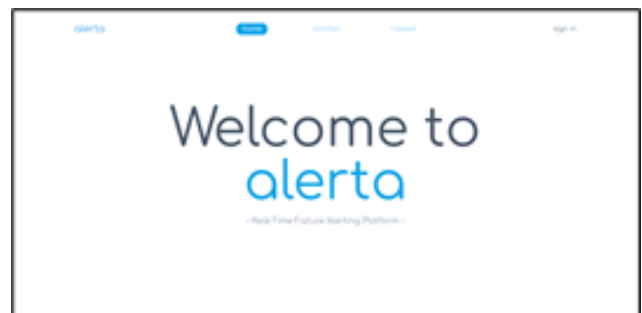


**Figure 19:** Home page display

The sign-in page is used for user authentication. It can be accessed by pressing the sign-in button on the right end of the navigation bar. Additionally, if the user forcibly accesses the monitor and history pages without authentication, the system will automatically redirect them to the sign-in page for authentication. This process requires two inputs: e-mail and password.



**Figure 20:** Sign-in page display

The monitor page displays information related to the VHF A/G equipment transmission readings received by the SDR. This page shows the attenuation value of the wave, the operating frequency, the transmission status, and the failure history for the current

month when the user accesses the application. Additionally, there is a chart displaying the accumulated failures that occurred each month over the past year.



**Figure 21:** Monitor page display

The history page functions to store all failure data that has occurred on the equipment. By default, the system displays failure data for the current month when the user accesses the application. However, users can select a date range for the failures they want to view using the provided range picker. Then, click the "Save as PDF" button to save the file.



**Figure 22:** Failure history display

### III. RESULTS AND DISCUSSION

#### i. Implementation

In this phase, the author conducted testing on the design developed in the development stage. The testing was performed using the VHF A/G R&S S4200 in the CNS Laboratory at the Indonesian Aviation Polytechnic in Curug on May 22, 2024. The tests were conducted on 10 aviation communication frequencies: 120.2 MHz, 125 MHz, 126.7 MHz, 127 MHz, 129.5 MHz, 130 MHz, 132.5 MHz, 133.2 MHz, 134 MHz, and 135 MHz.

The first step in testing was to prepare the RTL-SDR and Raspberry Pi devices. Turn on the Raspberry Pi by connecting the power supply to the power port on the Raspberry Pi. Ensure that the red indicator light on the Raspberry Pi is on, indicating no power input issues. Next, connect the antenna to the RTL-SDR and

connect the RTL-SDR to the Raspberry Pi through one of the USB ports on the Raspberry Pi.



**Figure 23:** RTL-SDR connection

On the VHF A/G R&S S4200, the PTT voltage can be sampled via the DB 25 breakout board at the back of the console desk. On this breakout board, pin 24 is PTT+ and pin 14 is ground. Connect pin 24 on the breakout board to the VBS pin on the INA226 sensor and pin 14 on the breakout board to the IN+ pin on the INA226 sensor through the socket on the PTT listener.

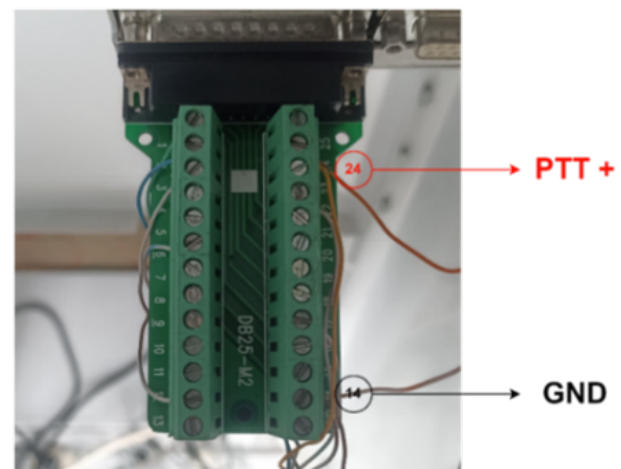


**Figure 24:** DB25 breakout board connection

After sampling the PTT voltage, turn on the PTT listener by connecting the ESP32 power port to an electrical terminal using a 5 VDC power supply. The PTT listener is ready when the green LED on the PTT listener blinks, indicating successful connection to WiFi and the Firebase server.

The last device to prepare is the alert system. Connect the ESP32 power port to an electrical terminal using a 5 VDC power supply to power the device. Wait until the connection process to WiFi and the Firebase server is complete, indicated by the blue LED on the bottom left of the alert system blinking.

Once all devices are ready, proceed to the testing phase. The first step is to set the operating frequency



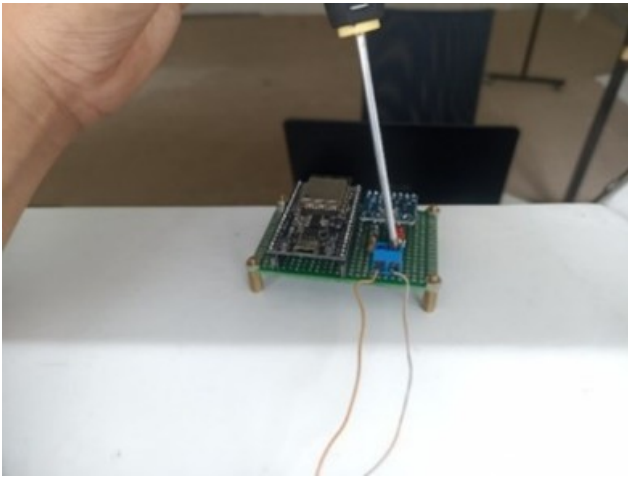


Figure 25: Breakout board connection to the PTT listener

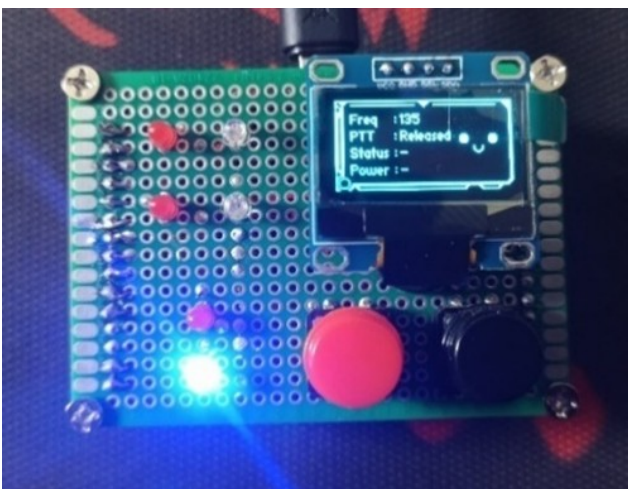


Figure 26: Alert system status when powered on

of the VHF A/G transmission. On the VHF A/G R&S S4200, this can be done by pressing the menu button on the front panel, selecting the operation menu, and clicking on frequency to change the operating frequency.



Figure 27: Set frequency on VHF A/G

Additionally, set the SDR operating frequency through the platform. Click the frequency button on the monitor page, enter the operating frequency in MHz, and click submit. Then, start the calibration process.

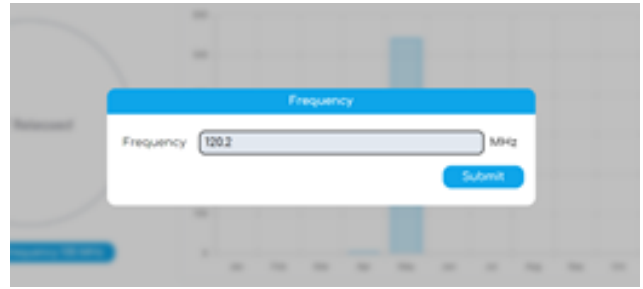


Figure 28: Set frequency on the platform

When the PTT is pressed, the calibration process will run for 10 seconds. During the first five seconds, provide information via the microphone such as a radio check. Then, hold the PTT button until the calibration process is complete.



Figure 29: Calibration process

After the calibration process is complete, the program will produce three values: the transmission power calibration value, the audio level calibration value, and the calibration status indicating that calibration has been performed. These values are sent to Firebase to be used as a reference during transmission monitoring.

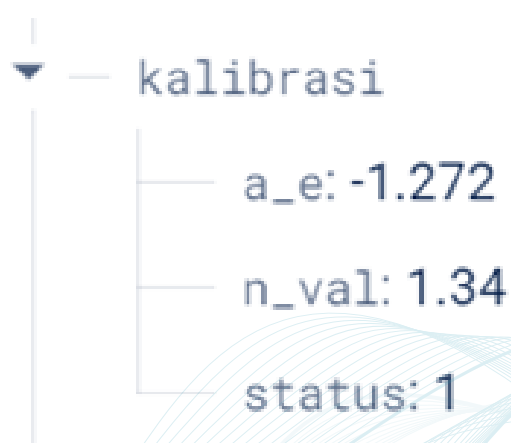


Figure 30: Calibration results on Firebase

Based on these values, a transmission can be con-

sidered normal if it meets the following two equations, where the variable  $RFK$  is the transmission power calibration value,  $LAK$  is the audio level calibration value,  $x$  is the received transmission power, and  $y$  is the received audio level.

$$10\log\left(\frac{x}{RFK}\right) > -3 \text{ dB} \quad (1)$$

$$y \geq LAK \quad (2)$$

The first test was reading the transmission power and status under normal conditions. This test was conducted by pressing the PTT button and providing voice information. According to equations (1) and (2), a transmission is considered normal if the attenuation is less than 3 dB and the audio level is greater than or equal to  $LAK$ .

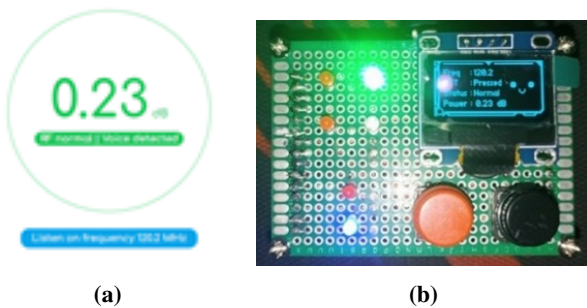


**Figure 31:** Design display during normal transmission test (a) on the platform (b) on the alert system

The second test was reading the transmission power and status when there was no information. This test was conducted by pressing the PTT button without providing information. According to equation (2), a transmission is considered to have no information if the audio level is less than  $LAK$ .

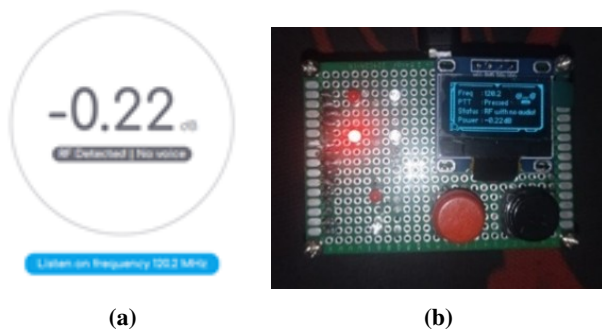


**Figure 32:** Design display during no-voice transmission test (a) on the platform (b) on the alert system

The third test was reading the transmission power and status when there was an RF power drop. According to equation (1), a transmission is considered abnormal if the attenuation is greater than or equal to 3 dB. This test was conducted by reducing the RF power

on the VHF A/G by setting the transmission power from normal (50 watts) to low (5 watts) through the operation menu on the VHF A/G R&S S4200. Press the PTT button to start the measurement after adjusting the RF power.

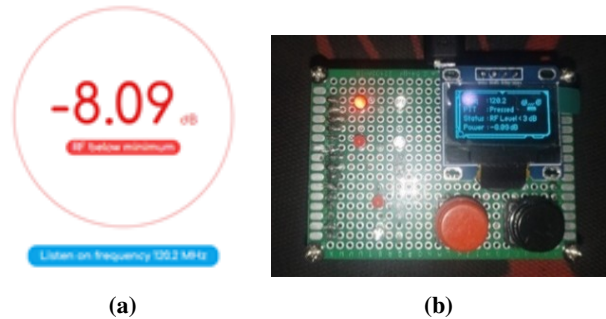


**Figure 33:** Design display during RF power drop test (a) on the platform (b) on the alert system

## ii. Evaluation

Based on the tests conducted, the design can receive modulated waves transmitted by the VHF A/G transmitter. These waves are processed to produce three values: transmission power (RFP), audio level (LA), and transmission status. All 10 tests successfully read the transmission power and audio level values according to the type of test performed. The following are the test results:

In this stage, the author conducted testing on the design developed during the development phase. The testing was conducted using the VHF A/G R&S S4200 at the CNS Laboratory of the Indonesian Aviation Polytechnic in Curug on May 22, 2024. The tests were carried out on 10 aviation communication frequencies: 120.2 MHz, 125 MHz, 126.7 MHz, 127 MHz, 129.5 MHz, 130 MHz, 132.5 MHz, 133.2 MHz, 134 MHz, and 135 MHz.

**Table 5:** Test Results for Normal Transmission

Freq. (MHz)	Calibration Results		Reading Results	
	LAK (dBm)	RFK (dBm)	LA (dBm)	RFP (dB)
120.2	-1.272	1.34	-0.3687	0.23
125	-1.102	1.084	-0.5862	-0.22
126.7	-1.13	0.646	-0.5587	0.89
127	-0.927	0.821	-0.7579	0.13
129.5	-0.914	0.21	-0.8334	0.82
130	-1.175	0.198	-0.6953	-0.38
132.5	-1.189	0.229	-0.8823	-0.5
133.2	-1.035	0.289	-0.4789	0.11
134	-1.274	0.401	-0.7217	0.11
135	-1.093	1.01	-0.8452	-0.29

During the normal transmission test, the design successfully displayed readings indicating that there was no significant attenuation in the transmission

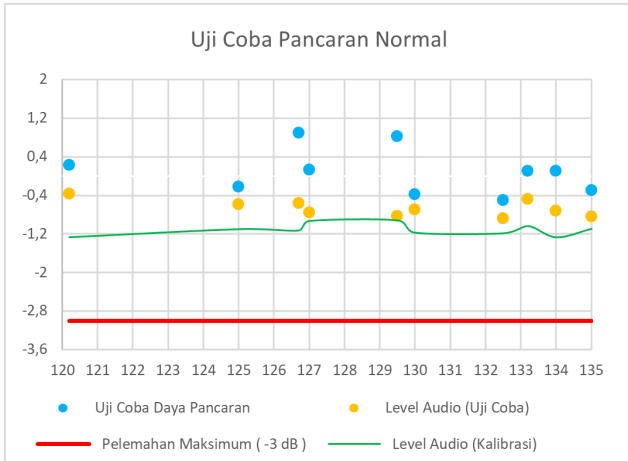


Figure 34: Test results for normal transmission

power, with the largest deviation being 0.89 dB and the smallest deviation being -0.5 dB. The attenuation in the transmission was categorized as normal because it was greater than -3 dB. The audio level readings confirmed that information was transmitted by the VHF A/G, as indicated by values greater than the audio calibration level. Additionally, both the platform and the alert system successfully displayed normal transmission indicators.

Table 6: Test Results for Transmission Without Information

Freq. (MHz)	Calibration Results		Reading Results	
	LAK (dBm)	RFK (dBm)	LA (dBm)	RFP (dB)
120.2	-1.272	1.34	-1.4825	-0.22
125	-1.102	1.084	-1.6448	0.9
126.7	-1.13	0.646	-1.5422	0.12
127	-0.927	0.821	-1.4515	-0.2
129.5	-0.914	0.21	-1.437	-0.57
130	-1.175	0.198	-1.628	0.34
132.5	-1.189	0.229	-1.5409	-0.53
133.2	-1.035	0.289	-1.618	0.46
134	-1.274	0.401	-2.0525	-0.92
135	-1.093	1.01	-1.5498	-0.22

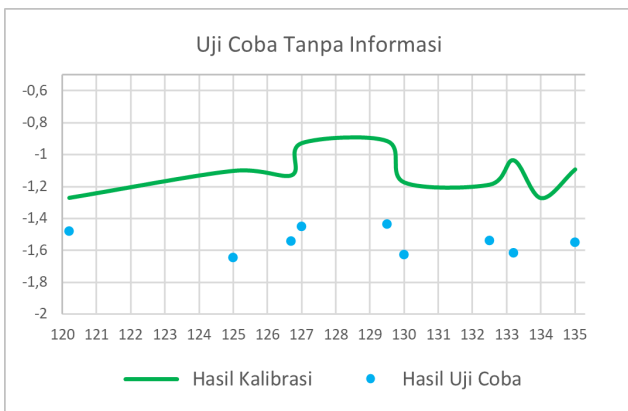


Figure 35: Test results for transmission without information

In the test for transmission without information,

the design successfully displayed readings indicating no information in the VHF A/G transmission. This was evidenced by audio level readings below the audio calibration level. As shown in Figure 35, the audio level readings were below the calibration threshold. Additionally, the platform and alert system successfully displayed alarm indicators.

Table 7: Test Results for RF Power Drop

Freq. (MHz)	Calibration Results		Reading Results	
	LAK (dBm)	RFK (dBm)	LA (dBm)	RFP (dB)
120.2	-1.272	1.34	-1.1146	-8.09
125	-1.102	1.084	-1.0878	-9.58
126.7	-1.13	0.646	-1.3051	-9.09
127	-0.927	0.821	-1.5735	-11.77
129.5	-0.914	0.21	-2.0044	-11.71
130	-1.175	0.198	-2.2442	-10.46
132.5	-1.189	0.229	-2.1849	-12.24
133.2	-1.035	0.289	-2.1648	-11.34
134	-1.274	0.401	-1.2206	-10.4
135	-1.093	1.01	-1.938	-11.0

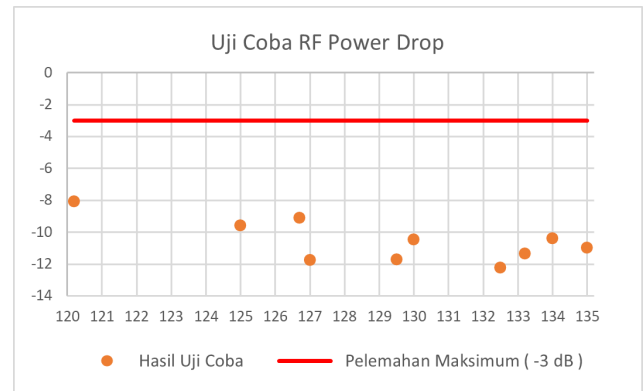


Figure 36: Test results for RF power drop

In the RF power drop test, the design successfully displayed readings indicating attenuation in the transmission. This was confirmed by transmission power readings below -3 dB, with the largest deviation being 2.24 dB and the smallest deviation being 0.4 dB. As shown in Figure 36, the transmission power readings were below -3 dB. Additionally, the platform and alert system successfully displayed alarm indicators.

Based on the testing results, the design met the design criteria as follows:

#### IV. CONCLUSION

Based on the tests conducted on 10 aviation frequencies, the design of the modulated wave transmission failure detection system for aviation communication using IoT-based RTL-SDR was able to receive modulated waves transmitted by VHF A/G. The received waves were then processed into transmission power values, audio levels, and transmission status. The measurement

**Table 8:** Design Criteria

No	Module	Component	Indicator	Status
1	SDR	RTL-SDR & Raspberry Pi	Can receive modulated waves at aviation frequencies	Compliant
			Can measure transmission power from received modulated waves	Compliant
			Can measure embedded audio level	Compliant
			Can determine transmission status based on processed data	Compliant
			Can send data to the server	Compliant
2	Alert System	ESP32 & Buzzer	Can receive data from the server	Compliant
			Can provide immediate warnings to technicians if the transmission status is fail	Compliant
			Can display transmission power, audio level, and transmission status	Compliant
3	PTT Listener	ESP32 & INA226 Sensor	Can receive PTT voltage and provide logic input values according to PTT button position to ESP32	Compliant
			Can send data to the server	Compliant
4	Software Device	Firebase	Can send and receive data in real-time	Compliant
			Can store data when the transmission status is fail	Compliant
5	Platform	Next JS	Has authentication	Compliant
			Can display transmission power	Compliant
			Can display transmission status	Compliant
			Can send and receive data from the server	Compliant
			Can display and save failure record data	Compliant

of transmission power yielded the largest deviation value of 2.24 dB and the smallest deviation value of 0.4 dB. This deviation occurred due to the receiving antenna's specifications differing from those of the VHF A/G transmitter antenna. Additionally, the design successfully provided warnings to technicians through the platform and alert system when communication failures occurred.

## REFERENCES

- [1] M. KAYA and S. S. ATEŞ, "The share of communication errors in aircraft accidents and artificial intelligences that can be developed based on communication in aviation," *International Journal of Entrepreneurship and Management Inquiries*, vol. 7, no. 12, pp. 82–95, Aug. 2023. [Online]. Available: <https://doi.org/10.55775/ijemi.1143651>
- [2] Indonesia, "Pp no 77 tahun 2012 tentang perum lppnpi," [www.djpp.depkuham.go.id](http://www.djpp.depkuham.go.id), 2012.
- [3] A. H. Asri and L. Lidyawati, "Analisis kinerja vhf-a/g tower/adc dengan vhf-a/g app di bandar udara husein sastranegara bandung," *TELKA - Telekomunikasi, Elektronika, Komputasi dan Kontrol*, vol. 4, no. 1, pp. 75–84, May 2018. [Online]. Available: <https://doi.org/10.15575/telka.v4n1.75-84>
- [4] K. Perhubungan, "Kp 103 tahun 2015 tentang standar teknis dan operasi (manual of standard casr 171-02) spesifikasi teknis fasilitas telekomunikasi penerbangan," Jakarta, 2015.
- [5] M. P. R. Indonesia, *Peraturan Menteri Perhubungan Republik Indonesia Nomor PM 48 Tahun 2017 Tentang Peraturan Keselamatan Penerbangan Sipil Bagian 171 (Civil Aviation Safety Regulation Part 171) Tentang Penyelenggara Pelayanan Telekomunikasi Penerbangan*, Indonesia, 2017.
- [6] T. Cahyani, O. Hendra, R. Sadiatmi, W. Nugraha, and M. F. Habillah, "Rancangan monitoring peralatan transmitter very high frequency pae t6t berbasis web server," *Journal of Airport Engineering Technology (JAET)*, vol. 1, no. 2, pp. 48–53, Apr. 2021. [Online]. Available: <https://doi.org/10.52989/jaet.v1i2.14>
- [7] A. L. G. Reis, A. F. Barros, K. G. Lenzi, L. G. P. Meloni, and S. E. Barbin, "Introduction to the software-defined radio approach," *IEEE Latin America Transactions*, vol. 10, no. 1, pp. 1156–1161, Jan. 2012. [Online]. Available: <https://doi.org/10.1109/TLA.2012.6142453>
- [8] S. Sotyohadi and I. B. Sulistiawati, "Desain low noise transceiver 7 mhz berbasis software defined radio (sdr)," *Jurnal Mnemonic*, vol. 2, no. 1, pp. 73–78, Dec. 2019. [Online]. Available: <https://doi.org/10.36040/mnemonic.v2i1.55>
- [9] H. Wijanto, "Design of software defined radio (sdr) in 88 mhz to 800 mhz multiband frequency based audio receipt system at raspberry," *Telekontran: Jurnal Ilmiah Telekomunikasi, Kendali dan Elektronika Terapan*, vol. 7, no. 2, Feb. 2020. [Online]. Available: <https://doi.org/10.34010/telekontran.v7i2.1749>
- [10] N. BniLam, D. Joosens, J. Steckel, and M. Weyn, "Low cost aoa unit for iot applications," in *2019 13th European Conference on Antennas and Propagation (EuCAP)*, 2019, pp. 1–5.
- [11] R. W. Stewart *et al.*, "A low-cost desktop software defined radio design environment using matlab, simulink, and the rtl-sdr," *IEEE Communications Magazine*, vol. 53, no. 9, pp. 64–71, Sep. 2015. [Online]. Available: <https://doi.org/10.1109/MCOM.2015.7263347>
- [12] Y. Molina-Tenorio, A. Prieto-Guerrero, and R. Aguilar-Gonzalez, "Real-time implementation of multiband spectrum sensing using sdr technology," *Sensors*, vol. 21, no. 10, p. 3506, May 2021. [Online]. Available: <https://doi.org/10.3390/s21103506>

- [13] B. B. Harianto, A. Irfansyah, and Y. Suprpto, "Low cost prototype simulation of spectrum analyzer base on gnu radio and rtl-sdr," in *IOP Conference Series: Materials Science and Engineering*, vol. 909, no. 1, Dec. 2020, p. 012011. [Online]. Available: <https://doi.org/10.1088/1757-899X/909/1/012011>
- [14] S. Majumder, "Energy detection spectrum sensing on rtl-sdr based iot platform," in *2018 Conference on Information and Communication Technology (CICT)*. IEEE, Oct. 2018, pp. 1–6. [Online]. Available: <https://doi.org/10.1109/INFOCOMTECH.2018.8722360>
- [15] H. Mohamed *et al.*, "Partial discharge detection using low cost rtl-sdr model for wideband spectrum sensing," in *2016 23rd International Conference on Telecommunications (ICT)*. IEEE, May 2016, pp. 1–5. [Online]. Available: <https://doi.org/10.1109/ICT.2016.7500353>
- [16] P. L. C. Yogyakarta, "Standar operasional prosedur (sop) pelayanan telekomunikasi penerbangan perum lppnpi cabang yogyakarta," 2021.
- [17] G. Muruganantham, "Developing of e-content package by using addie model," *International Journal of Applied Research*, vol. 1, no. 3, pp. 52–54, 2015.
- [18] G. Fortino *et al.*, "Towards multi-layer interoperability of heterogeneous iot platforms: The inter-iot approach," in *Lecture Notes in Computer Science*, 2018, pp. 199–232. [Online]. Available: [https://doi.org/10.1007/978-3-319-61300-0\\_10](https://doi.org/10.1007/978-3-319-61300-0_10)
- [19] A. Alsalemi *et al.*, "Real-time communication network using firebase cloud iot platform for ecmo simulation," in *2017 IEEE International Conference on Internet of Things (iThings), Green Computing and Communications (GreenCom), Cyber, Physical and Social Computing (CPSCom), Smart Data (SmartData)*. IEEE, Jun. 2017, pp. 178–182. [Online]. Available: <https://doi.org/10.1109/iThings-GreenCom-CPSCom-SmartData.2017.31>
- [20] C. Khawas and P. Shah, "Application of firebase in android app development-a study," *International Journal of Computer Applications*, vol. 179, no. 46, pp. 49–53, Jun. 2018. [Online]. Available: <https://doi.org/10.5120/ijca2018917200>
- [21] A. Albiol, A. Corbi, and D. Burgos, "Design of a remote signal processing student lab," *IEEE Access*, vol. 5, pp. 16 068–16 076, 2017. [Online]. Available: <https://doi.org/10.1109/ACCESS.2017.2736165>